

Unrestricted solution of the Elishberg equations for Nb

Autor(en): **Peter, M. / Ashkenazi, J. / Dacorogna, M.**

Objektyp: **Article**

Zeitschrift: **Helvetica Physica Acta**

Band (Jahr): **50 (1977)**

Heft 2

PDF erstellt am: **10.08.2024**

Persistenter Link: <https://doi.org/10.5169/seals-114856>

Nutzungsbedingungen

Die ETH-Bibliothek ist Anbieterin der digitalisierten Zeitschriften. Sie besitzt keine Urheberrechte an den Inhalten der Zeitschriften. Die Rechte liegen in der Regel bei den Herausgebern.

Die auf der Plattform e-periodica veröffentlichten Dokumente stehen für nicht-kommerzielle Zwecke in Lehre und Forschung sowie für die private Nutzung frei zur Verfügung. Einzelne Dateien oder Ausdrucke aus diesem Angebot können zusammen mit diesen Nutzungsbedingungen und den korrekten Herkunftsbezeichnungen weitergegeben werden.

Das Veröffentlichen von Bildern in Print- und Online-Publikationen ist nur mit vorheriger Genehmigung der Rechteinhaber erlaubt. Die systematische Speicherung von Teilen des elektronischen Angebots auf anderen Servern bedarf ebenfalls des schriftlichen Einverständnisses der Rechteinhaber.

Haftungsausschluss

Alle Angaben erfolgen ohne Gewähr für Vollständigkeit oder Richtigkeit. Es wird keine Haftung übernommen für Schäden durch die Verwendung von Informationen aus diesem Online-Angebot oder durch das Fehlen von Informationen. Dies gilt auch für Inhalte Dritter, die über dieses Angebot zugänglich sind.

Unrestricted solution of the Eliashberg equations for Nb

by M. Peter, J. Ashkenazi and M. Dacorogna

Département de Physique de la Matière Condensée
 Université de Genève, Suisse

(25. VIII. 1976)

Abstract. The Eliashberg equations for superconductivity are solved numerically for Nb using band structure results and experimental phonon spectrum. The solution is done unrestrictedly in the sense that all anisotropy effects as well as the frequency dependence of the gap function are treated correctly. The electron-phonon coupling constants are evaluated in the rigid-ion approximation, and the Coulomb interaction is treated on the same level using typical parameters. The method used requires reasonable computer time which could make it applicable for rather complicated materials. The anisotropy effects on the gap function and T_c are studied with some detail.

1. Introduction

Right after the BCS theory had been proposed for superconductivity, there arose the problem how to treat superconductors with strong electron-phonon and Coulomb interactions. Nambu [1] has applied the Green's functions method for superconductivity to tackle this problem, and Eliashberg [2] obtained in terms of this method a set of equations called after his name. Those equations were generalized for the finite temperature case by Scalapino et al. [3] and are given in the Matsubara representation in equations (1)

$$\chi(\mathbf{k}, n) = -\frac{1}{\beta} \sum_{\mathbf{k}'n'} \frac{[\varepsilon_{\mathbf{k}'} + \chi(\mathbf{k}', n')][D(\mathbf{k}, \mathbf{k}', n - n') - V(\mathbf{k}, \mathbf{k}')] }{[\omega_{n'} Z(\mathbf{k}', n')]^2 + [\varepsilon_{\mathbf{k}'} + \chi(\mathbf{k}', n')]^2 + \phi(\mathbf{k}', n')^2} \quad (1a)$$

$$Z(\mathbf{k}, n) = 1 + \frac{1}{\beta\omega_n} \sum_{\mathbf{k}'n'} \frac{\omega_{n'} Z(\mathbf{k}', n')D(\mathbf{k}, \mathbf{k}', n - n')}{[\omega_{n'} Z(\mathbf{k}', n')]^2 + [\varepsilon_{\mathbf{k}'} + \chi(\mathbf{k}', n')]^2 + \phi(\mathbf{k}', n')^2} \quad (1b)$$

$$\phi(\mathbf{k}, n) = \frac{1}{\beta} \sum_{\mathbf{k}'n'} \frac{\phi(\mathbf{k}', n')[D(\mathbf{k}, \mathbf{k}', n - n') - V(\mathbf{k}, \mathbf{k}')] }{[\omega_{n'} Z(\mathbf{k}', n')]^2 + [\varepsilon_{\mathbf{k}'} + \chi(\mathbf{k}', n')]^2 + \phi(\mathbf{k}', n')^2} \quad (1c)$$

The notations are the ones adopted previously [4, 5, 6].

Since we are dealing with a multi-band problem, the \mathbf{k} index is followed by a band index b which is omitted here (and generally also later on). Non-diagonal band terms on the right sides of the equations are ignorable provided that correlation energies are small compared with Hartree-Fock energies. $\chi(\mathbf{k}, n)$ is the ordinary self-energy term, its dependence on n can be generally ignored for Matsubara frequencies involved in superconductivity (except for special cases as for instance charge density waves), replacing $\varepsilon_{\mathbf{k}} + \chi(\mathbf{k}, n)$ by $\bar{\varepsilon}_{\mathbf{k}}$ (and omitting the bar). $Z(\mathbf{k}, n)$ is the mass renormalization, and $\phi(\mathbf{k}, n)/Z(\mathbf{k}, n)$ plays the role of the superconducting gap (for imaginary frequencies).

Various attempts have been made to treat those equations. McMillan [7], neglecting high frequency contributions and anisotropy in \mathbf{k} -space, obtained a semi-empirical equation for T_c . The idea of the semiempirical equation has been developed further by several people. Birnboim and Gutfreund [8], starting from the Appel-Kohn [9] formalism, appropriate for tightly bound electrons, could fit their results with a similar formula. Allen and Dynes [10] and others solved the Eliashberg equations neglecting anisotropy. Butler and Allen [11] made a calculation approximating the electron anisotropy by Fermi surface harmonics and neglecting phonon anisotropy.

In the present work the linearized Eliashberg equations (which hold for $T \cong T_c$) are solved unrestrictedly, namely obtaining the correct frequency dependence and treating anisotropy almost exactly both for the electrons and for the phonons. Here the method and the results are discussed briefly; the detailed work will be described later.

2. Formalism

As was discussed in Reference [10], the mass renormalization and the gap are invariant under the transformation $n \rightarrow -n - 1$, so that the n' summation in equations (1) can be limited to non-negative values.

Similarly to Reference [3], it can be shown that this summation is cut off at n_c , such that $\omega_c \equiv \omega_{n_c} \gg \theta_D$, provided that the Coulomb potential matrix \mathbf{V} is replaced by a pseudo potential matrix \mathbf{U} given by:

$$\mathbf{U} = (\mathbf{1} + \mathbf{\Omega})^{-1} \mathbf{V} \quad (2a)$$

where

$$\Omega(\mathbf{k}, \mathbf{k}') = V(\mathbf{k}, \mathbf{k}') E_{\mathbf{k}'}(n_c) \quad (2b)$$

$$E_{\mathbf{k}}(n_c) = \frac{1}{2|\varepsilon_{\mathbf{k}}|} \left[1 - \frac{2}{\pi} \arctg \left| \frac{\omega_c}{\varepsilon_{\mathbf{k}}} \right| \right] \begin{cases} \xrightarrow{\varepsilon_{\mathbf{k}} \ll \omega_c} 0 \\ \xrightarrow{\varepsilon_{\mathbf{k}} \gg \omega_c} \frac{1}{2|\varepsilon_{\mathbf{k}}|} \end{cases} \quad (2c)$$

(Band indices are omitted here.)

Integrating normal to the Fermi surface by using the residuum theorem, the sum over \mathbf{k}' in equations (1) can be replaced for $\theta_D \ll E_F$ by a sum over the Fermi surface (FS). As was discussed in Reference [6], the FS summation can be limited to the irreducible Brillouin zone (BZ) provided that \mathbf{D} and \mathbf{U} are replaced by \mathbf{D}^* and \mathbf{U}^* defined by:

$$D^*(\mathbf{k}, \mathbf{k}', n) = \sum_s D(\mathbf{k}, s\mathbf{k}', n); \quad U^*(\mathbf{k}, \mathbf{k}') = \sum_s U(\mathbf{k}, s\mathbf{k}') \quad (3)$$

where s are the 48 star operations spanning the whole BZ out of the irreducible one.

Each \mathbf{k} represents in our calculation a piece of the IFS (irreducible Fermi surface). All averaging procedures are reduced to within such a piece (compared to the whole FS or BZ in theories neglecting anisotropy), each such a piece has a weight $W_{\mathbf{k}}$ which is the density of states integrated over it. Equations (1) reduce then to:

$$Z(\mathbf{k}, n) = 1 + \frac{\pi}{\beta\omega_n} \sum_{\substack{0 \leq n' \leq n_c \\ \mathbf{k}' \in \text{IFS}}} W_{\mathbf{k}'} [D^*(\mathbf{k}, \mathbf{k}', n - n') - D^*(\mathbf{k}, \mathbf{k}', n + n' + 1)] \quad (4a)$$

$$\phi(\mathbf{k}, n) = \sum_{\substack{0 \leq n' \leq n_c \\ \mathbf{k}' \in \text{IFS}}} A(\mathbf{k}n, \mathbf{k}'n') \phi(\mathbf{k}'n') \quad (4b)$$

where

$$A(\mathbf{k}n, \mathbf{k}'n') = \frac{\pi}{\beta\omega_n} \frac{W_{\mathbf{k}'}}{Z(\mathbf{k}', n')} \cdot [D^*(\mathbf{k}, \mathbf{k}', n - n') + D^*(\mathbf{k}, \mathbf{k}', n + n' + 1) - 2U^*(\mathbf{k}, \mathbf{k}')] \quad (4c)$$

Equation (4b) has a non-trivial solution for:

$$\det [\mathbf{1} - \mathbf{A}] = 0 \quad (5)$$

(those are matrices both in the \mathbf{k} and the n indices).

The highest temperature in which equation (5) is satisfied is T_c . Using the Wilkinson method [12], the gap function $\phi(\mathbf{k}, n')$ is obtained easily when this determinant is evaluated close to a zero value.

3. Calculation

In order to solve equation (5) (which is relatively rapid), the following calculations have to be done:

First we need a band structure yielding a reasonable Fermi surface. We have used the results obtained for Nb by Mattheiss [13] in the APW method (whose FS has been verified experimentally). The band structure has been fitted by effective tight-binding integrals using 6×6 tight binding matrices for the hybridized 4d-5s bands around E_F .

Effective crystal field and transfer integrals were determined up to the third shell. The transfer integrals were calculated in the two-centre approximation using a distance-dependent parametrization developed from the method of Ashkenazi and Weger [14].

Ten independent band parameters were required, yielding a band structure close to the one of Mattheiss (particularly near the Fermi surface). Some difficulty in the exact fit appeared due to a 5p type level lying not far from E_F near the N symmetry point. The results obtained for the band integrals are shown in Table I, and for the irreducible Fermi surface in Figure 1. This IFS is composed of a jungle gym, ellipsoid and jack portions like the one of Mattheiss, and in order to solve the Eliashberg equations, it is divided into 22 pieces shown in the graph.

In order to obtain those pieces, we started with a cubic mesh of 2109 points in the IBZ. 492 points were calculated in which the axes of this mesh cut the FS. Those points were subdivided into 22 groups (FS pieces) using the criterion that the points within each piece are close both in their \mathbf{k} value and energy gradient. Making a FS integration, the density of states at E_F was found to be 9.9 states/(ryd-atom-spin) which is close to the one of Mattheiss (the density of states curves are also similar).

The surface and volume integrations required in this work were done using a new interpolation method, based inherently on equienergetical surfaces, which made the calculations rather simple compared to other interpolation methods. This method will be discussed elsewhere. The mesh used was found sufficient up to a high accuracy.

Table I
Values, in ryd, of the crystal field splitting, the Slater–Koster transfer integrals and their distance (R) derivatives, used for Nb in this work.

	R	$dd\sigma$	$dd\pi$	$dd\delta$	$ss\sigma$	$sd\sigma$	$K_{ds}^a)$	$K_{et}^b)$
	0						-0.06477	-0.09957
Integral $f(R)$	$a_0\sqrt{3}/2$	-0.08570	0.07909	-0.02452	-0.07288	-0.06892		
	$a_0^c)$	-0.04809	0.04168	-0.01183	-0.04959	-0.05064		
	$a_0\sqrt{2}$	-0.01035	0.00741	-0.00167	-0.01664	-0.01818		
Deriva- tive $\frac{R}{f} \frac{df}{dR}$	$a_0\sqrt{3}/2$	-3.922	-4.325	-4.921	-2.559	-1.879		
	a_0	-4.118	-4.588	-5.218	-2.800	-2.394		
	$a_0\sqrt{2}$	-4.806	-5.430	-6.136	-3.456	-3.517		

a) Crystal field splitting between the $4d$ and the $5s$ orbitals.

b) Crystal field splitting between the e ($d_{z^2}, d_{x^2-y^2}$) and the t (d_{xy}, d_{xz}, d_{yz}) orbitals.

c) $a_0 = 6.2294$ (a.u.).

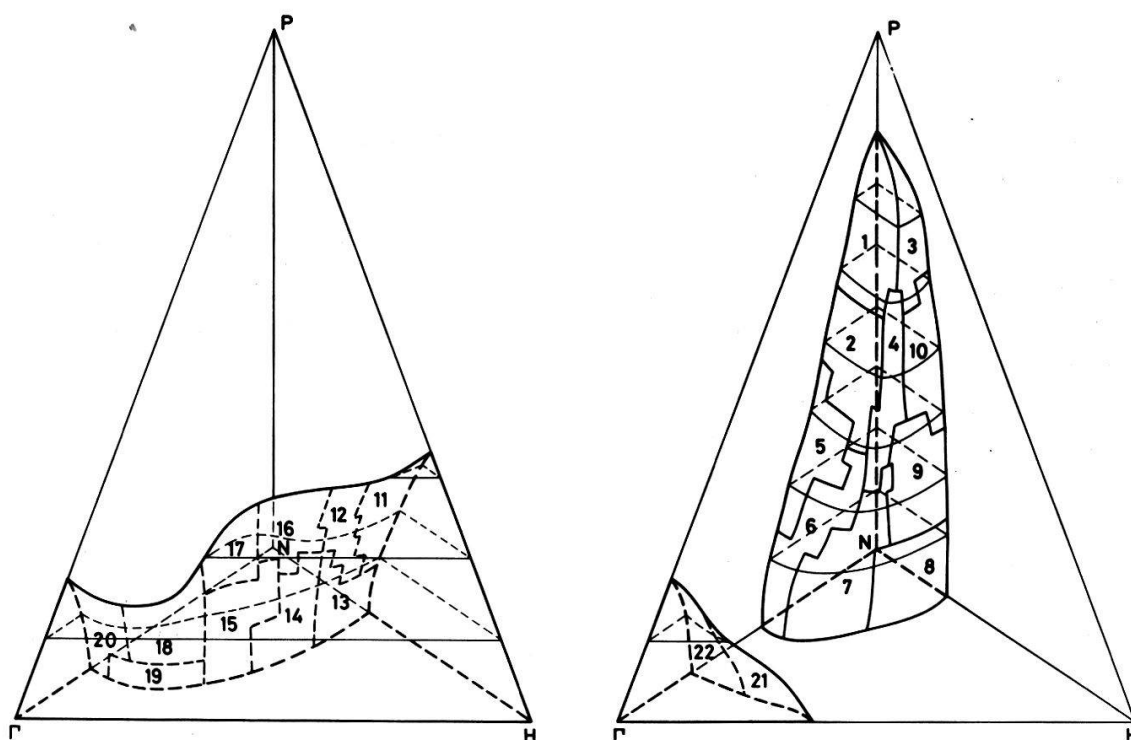


Figure 1

The irreducible Fermi surface of Nb obtained fitting our band parameters to the results of Mattheiss [13]. It is divided into 22 pieces for the solution of the Eliashberg equations. Pieces 1–10 form the ‘ellipsoid’, 11–20 form the ‘jungle-gym’ and 21–22 the ‘jack’.

In order to obtain the electron–phonon–electron interaction matrix $D^*(\mathbf{k}, \mathbf{k}', n - n')$, one needs values for the electron–phonon coupling constants and the phonon energies. The electron–phonon coupling is evaluated in the rigid ion approximation. Expressions for the coupling constants in terms of the Hamiltonian’s derivatives are given in References [4, 6]. The derivatives of the transfer integrals are obtained easily from their distance-dependent parametrization and shown in Table I. This method for the electron–phonon coupling is basically similar to the one used by

Birnbom and Gutfreund [8]. It has been shown [15] to account for the Mathias rules and the pressure dependence of T_c in transition metals. The tight-binding distance-dependence parametrization is known to be equivalent to the ones derived from the KKR method [16, 17]. For the case of d electrons it turns out to be close to R^{-5} behaviour, which is similar to Pettifor's results [18].

The phonon energies for each point in the BZ are calculated using Born-von Karman parameters obtained by Nagakawa and Woods [19] from neutron diffraction results.

Within each Fermi surface piece, the Hamiltonian space derivatives, needed for the evaluation of the electron-phonon coupling, are averaged using the original 492 points on the IFS. An average \mathbf{k} point is taken for each piece to evaluate eigenvectors and phonon energies.

In order to satisfy the star summation (equation 3), one has to evaluate coupling constants and phonon energies between each piece \mathbf{k} in the IFS, and a piece \mathbf{k}' in the whole FS. For the phonons, only 3×3 matrix diagonalizations are required, and their energies between all those pieces are calculated rapidly. (One can also calculate phonon energies for a mesh in the BZ and make a linear interpolation to $\mathbf{k}' - \mathbf{k}$). For the electron-phonon coupling on the other hand, rather simple star rules have been found, which enable us to diagonalize the electron 6×6 matrix just for the case where both \mathbf{k} and \mathbf{k}' are in the IFS, and then to obtain the results for the star of \mathbf{k}' by simple transformations. Special treatment has been made for a coupling of a piece with itself. (The numbers required for the Eliashberg equations are found to converge to finite values for $|\mathbf{k}' - \mathbf{k}| \rightarrow 0$.)

The Coulomb pseudopotential matrix $U^*(\mathbf{k}, \mathbf{k}')$ was treated on the same level as the \mathbf{D} matrix using again the above mentioned star rules. Since the Coulomb potential is screened, we consider only intra-atomic interactions as was generally done in similar calculations [3]. Similarly to a calculation done recently by Ashkenazi and Weger [20] for the metal-insulator transition in V_2O_3 and Ti_2O_3 , the interaction is expressed in terms of a matrix $\langle m_1 m_2 | V | m_3 m_4 \rangle$, where m_i are the $4d-5s$ orbitals (for intra-atomic interactions V is independent of \mathbf{k}).

The Coulomb matrix is expressed in terms of six parameters: Three parameters A, B, C for the $d-d$ interactions [21], whose relation to the Slater integrals is given by: $A = F^{(0)} - \frac{1}{9}F^{(4)}$; $B = \frac{1}{49}F^{(2)} - \frac{5}{441}F^{(4)}$; $C = \frac{5}{63}F^{(4)}$; two parameters D and E for the direct and exchange $s-d$ interactions; and one parameter F for the $s-s$ interaction. Since complicated screening effects play an important role in the determination of those parameters, it is difficult to evaluate them from first principles. So we have chosen for them the typical values:

$$A, B, C, D, E, F = 0.08, 0.003, 0.001, 0.02, 0.002, 0.01 \text{ ryd}$$

and studied the sensitivity of the results to their variation.

It is found that in the orbital (m) representation \mathbf{k} independent V yields also a \mathbf{k} independent U . So equation (2a) for the evaluation of U turns out to be a 36×36 matrix inversion problem, and the U matrix in this approximation is a generalized Morel-Anderson [22] pseudopotential. BZ integration is done evaluating Ω for that equation, and the calculated U is transformed from the orbital representation to $U^*(\mathbf{k}, \mathbf{k}')$. It is found that the pseudopotential's dependence on the Coulomb parameters is weak for the reasonable values range (saturation is obtained for $|\Omega| \gg 1$).

Next we solve the Eliashberg equations. It turns out that the highest temperature

where equation (5) is satisfied (i.e. T_c) is well separated from any other possible solution. Making an interpolation of the determinant's value to zero, convergence is obtained in a few steps. Z , D^* , U^* and A have to be calculated for each value of the trial temperature, however, most of the numbers required for the calculation are evaluated once and for all and stored, and each trial temperature requires a few minutes of computer time, on a UNIVAC 1108.

It is found that the electron-phonon coupling constants determined by our method are probably too large, and have to be multiplied by a factor of 0.7 (which means a factor of 0.49 in the electron-phonon-electron interaction) in order to obtain the observed T_c . This discrepancy could be a result of the rigid ion approximation [8, 17]. The dependence of T_c on the Coulomb parameters is weak for reasonable values as was noted before.

It turned out that for 22 pieces in the IFS, the maximal number of non-negative Matsubara frequencies permitted by the size of our computer was 14 ($n_c = 13$) yielding a value of 9.48°K for T_c . However, we found a criterion under which we could join pieces to reduce their number with a minimal effect on the resulting T_c .

It is based on the following:

A result of equation (4b) is that if there is a group of pieces Q such that for each $\mathbf{k}_1, \mathbf{k}_2 \in Q$ and for all n , $\phi(\mathbf{k}_1, n) = \phi(\mathbf{k}_2, n)$, then all the pieces in Q can be joint. Generally such an identity does not exist, however joining pieces with close $\phi(\mathbf{k}, n)$ should not be a bad approximation. The joining is done under the following renormalization equations:

$$W_Q D^*(Q, Q', n) = \sum_{\mathbf{k}' \in Q'} W_{\mathbf{k}'} \langle D^*(\mathbf{k}, \mathbf{k}', n) \rangle_{\mathbf{k} \in Q} \quad (6a)$$

$$W_Q U^*(Q, Q') = \sum_{\mathbf{k}' \in Q'} W_{\mathbf{k}'} \langle U^*(\mathbf{k}, \mathbf{k}') \rangle_{\mathbf{k} \in Q} \quad (6b)$$

In order to find out what pieces are to be joint, we have to get an idea about the behaviour of $\phi(\mathbf{k}, n)$. This can be done by two methods:

The first one is to calculate $\phi(\mathbf{k}, n)$ for n_c low enough, to keep the calculation within the computer's limitations. The low n gap functions are the most important ones for the pieces-joining criterion. The second method is to start from model functions $\tilde{\phi}(\mathbf{k}, n)$ which have a close behaviour to $\phi(\mathbf{k}, n)$, and multiply them by the A matrix as in equation (4b) replacing ϕ in the right side by $\tilde{\phi}$ (this can be done without keeping the matrix A itself which may be too large for the computer). The functions obtained then are closer to $\phi(\mathbf{k}, n)$, and can be used as a measure for the joining criterion. In each temperature iteration stage, we use functions obtained from those of the last stage by multiplying A .

It is found that suitable model functions to start with are:

$$\tilde{\phi}(\mathbf{k}, n) = \frac{\langle D^*(\mathbf{k}, \mathbf{k}', 0) \rangle_{\mathbf{k}'}}{Z(\mathbf{k}, n) \left[1 + \left(1 - \left\langle \frac{D^*(\mathbf{k}, \mathbf{k}', 1)}{D^*(\mathbf{k}, \mathbf{k}', 0)} \right\rangle_{\mathbf{k}'} \right)^n \right]^2} - \langle U^*(\mathbf{k}, \mathbf{k}') \rangle_{\mathbf{k}'} \quad (7)$$

The functions obtained multiplying them by A deviate only by about 1% from the exact gap functions.

Each one of the original 22 pieces \mathbf{k} is given a 'coordinate' $\phi(\mathbf{k}, n)$ in a n_0 dimensional space ($n_0 \leq n_c$, is chosen small enough to keep the behaviour of $\phi(\mathbf{k}, n_0)$ sensitive to D^*) and a 'mass' $W_{\mathbf{k}}$. Pieces which are close in this space are joint. The

best criterion found for the joining was to select the groups of pieces in such a way that the sum of their 'moments of inertia' around their 'centres of mass' would be minimalized.

4. Results

We studied the variation of T_c with the number of (aggregate) pieces, and the results (for $n_c = 13$) are shown in Figure 2. The anisotropy effect on T_c , defined as its variation between the infinite number of pieces, and the one piece cases, turns out to be an increase of 0.24°K , compared to the 0.06°K increase found by Butler and Allen [11]. About 60% of the anisotropy effect are obtained by two pieces and for 11 pieces there is only a 0.002°K deviation from the 22 pieces case.

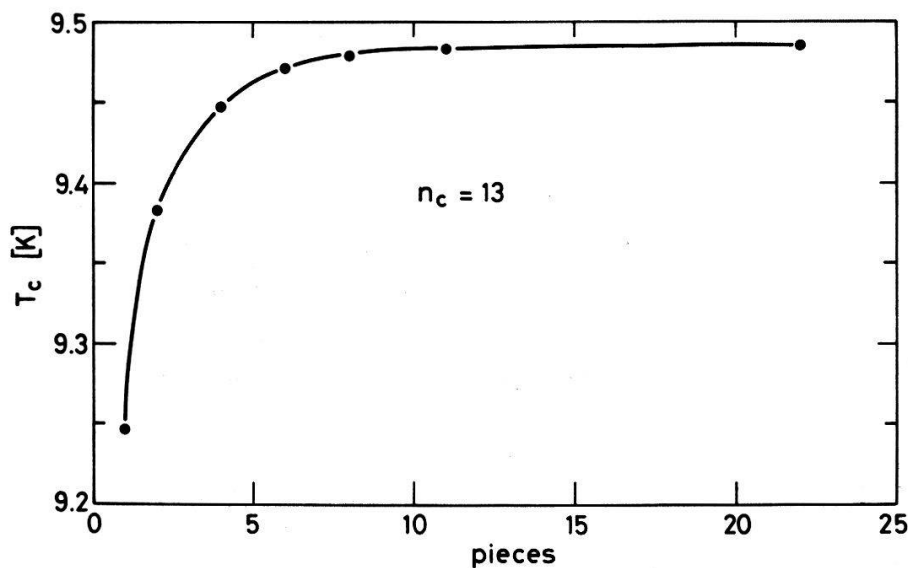


Figure 2

The variation of T_c with the number of groups (aggregate pieces) formed of the 22 ones in the IFS shown in Figure 1. The cut-off Matsubara frequency n_c is taken to be 13.

Using 11 aggregate pieces we could increase the cut-off Matsubara frequency n_c (due to the computer's limitation) up to 24. This increase had almost no effect on the anisotropy curve (Fig. 2) except for a constant shift of T_c . In Figure 3a the variation of T_c with n_c (for 11 pieces) is shown. T_c converges exponentially to the infinite cut-off case which is found, using a semi-logarithmic scale (Fig. 3b), to be $8.78 \pm 0.005^\circ\text{K}$.

In Tables II and III, the mass renormalization function $Z(\mathbf{k}, n)$ and the gap function $\phi(\mathbf{k}, n)$ are shown for $n_c = 24$. ϕ is defined here up to a multiplicative factor. It is calculated for the original 22 pieces, multiplying $\tilde{\phi}$ given in equation (7) by \bar{A} several times. We see that ϕ is converging into the high frequency limit (which is determined by the Coulomb interaction). The \mathbf{k} anisotropy is found to behave similarly for Z and for ϕ .

In Table IV we represent the joining of the original 22 pieces for the cases shown in Figure 2. It turns out that neighbouring ones (Fig. 1) are generally joint first. Using those results, one can study the nature of the anisotropy. Two important anisotropy effects are noticed. The first, determined by the electrons, yields both for zero frequency and high frequencies greater gap functions for pieces on the jungle-

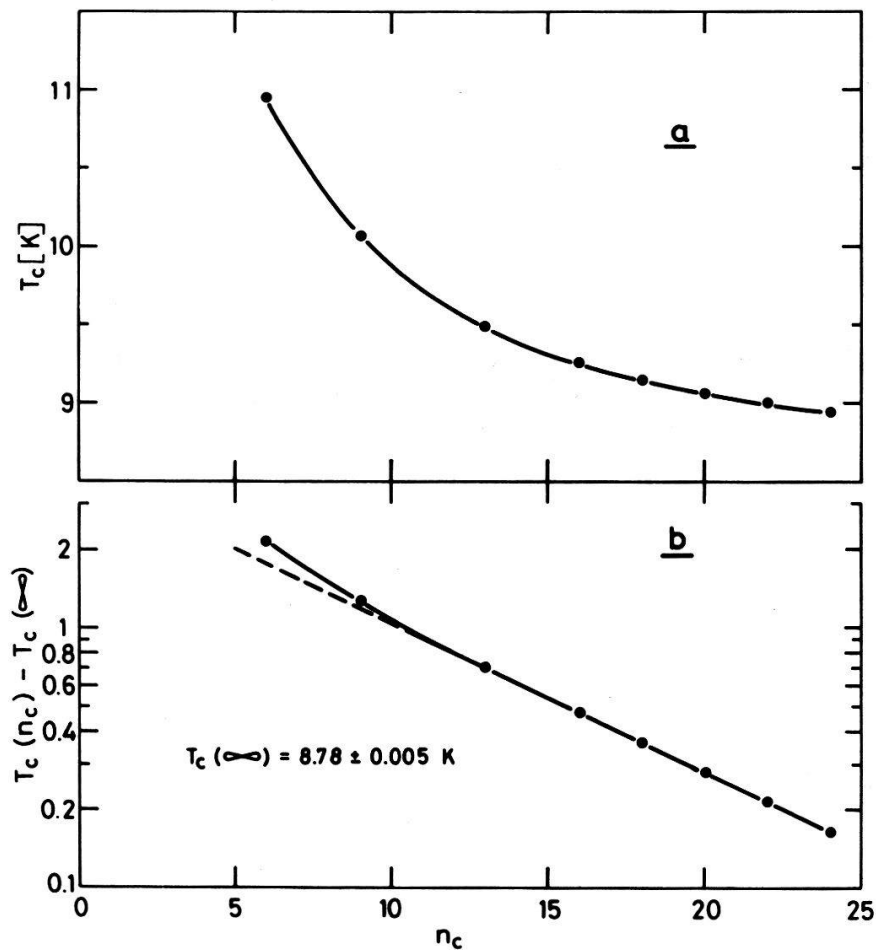


Figure 3a

The variation of T_c with the cut-off Matsubara frequency n_c for 11 aggregate pieces in the IFS.

Figure 3b

The same graph shown for $T_c - 8.78^\circ\text{K}$ on a semi-logarithmic scale.

gym and the jack, than for pieces on the ellipsoid. This is primarily an interference effect due to overlap of wave functions, occurring in the star summations (the same anisotropy is found both for \mathbf{D}^* and for \mathbf{U}^*). The wave functions on the jungle-gym and the jack are mainly admixture (with close amplitudes) of d_{xy} , d_{xz} and d_{yz} , while those on the ellipsoid contain also d_{z^2} and $d_{x^2-y^2}$, and the first yield a more constructive interference. Also, the wave functions on the ellipsoid contain generally a greater $5s$ component (which has lower Coulomb and electron-phonon interaction) than those on the jungle-gym and the jack, but this is found to be a secondary effect.

The second anisotropy effect is due to the phonons, and results in a faster decrease with frequency of the gap functions on pieces which have other pieces in their close neighbourhood. The phonons connecting close pieces are soft, resulting in a fast decrease with frequency of the \mathbf{D} matrix elements between them.

In the one (aggregate) piece result shown in Figure 2, there is still some anisotropy effect through the construction of the \mathbf{D}^* matrix. In order to make a comparison with the 'total' isotropic approximation, we calculated the McMillan parameters [7], making a weighted average of our pseudopotential, and the usual McMillan electron-phonon function over the FS pieces. We obtained $\lambda = 0.857$, $\mu^* = 0.111$, which are close to the values predicted by McMillan, and using his semiempiric formula one obtains $T_c = 9.04^\circ\text{K}$.

Table II
The mass renormalization function $Z(\mathbf{k}, n)$ for 22 IFS pieces (horizontal). 25 non-negative Matsubara frequencies (vertical) are considered ($n_c = 24$).

n	1	2	3	4	5	6	7	8	9	10	11	12	13	14	15	16	17	18	19	20	21	22
0	1.58	1.64	1.57	1.65	1.70	1.74	1.72	1.65	1.64	1.61	2.07	1.98	1.89	1.93	1.95	1.89	1.89	1.95	1.94	1.92	1.98	1.92
1	1.55	1.60	1.53	1.61	1.65	1.69	1.67	1.61	1.60	1.57	2.01	1.92	1.83	1.86	1.86	1.82	1.81	1.83	1.81	1.79	1.87	1.80
2	1.50	1.55	1.48	1.55	1.59	1.62	1.61	1.55	1.54	1.52	1.93	1.84	1.76	1.77	1.77	1.74	1.73	1.72	1.70	1.68	1.77	1.69
3	1.45	1.49	1.43	1.50	1.53	1.56	1.55	1.50	1.49	1.47	1.84	1.76	1.69	1.69	1.68	1.66	1.64	1.63	1.61	1.59	1.68	1.60
4	1.40	1.44	1.38	1.45	1.48	1.50	1.49	1.45	1.44	1.42	1.76	1.68	1.62	1.62	1.60	1.59	1.57	1.56	1.53	1.52	1.60	1.52
5	1.36	1.40	1.35	1.41	1.43	1.45	1.44	1.41	1.40	1.38	1.68	1.61	1.56	1.56	1.54	1.53	1.51	1.50	1.47	1.46	1.54	1.46
6	1.33	1.36	1.31	1.37	1.39	1.41	1.40	1.37	1.36	1.34	1.62	1.56	1.51	1.50	1.49	1.48	1.46	1.45	1.43	1.41	1.48	1.41
7	1.30	1.33	1.29	1.34	1.36	1.37	1.37	1.34	1.33	1.31	1.57	1.51	1.46	1.46	1.44	1.44	1.42	1.40	1.38	1.37	1.44	1.37
8	1.27	1.30	1.26	1.31	1.33	1.34	1.34	1.31	1.30	1.29	1.52	1.46	1.42	1.42	1.40	1.40	1.38	1.37	1.35	1.34	1.40	1.34
9	1.25	1.28	1.24	1.28	1.30	1.32	1.31	1.28	1.28	1.26	1.48	1.43	1.39	1.39	1.37	1.37	1.35	1.34	1.31	1.29	1.34	1.29
10	1.23	1.26	1.22	1.26	1.28	1.29	1.29	1.26	1.26	1.24	1.44	1.40	1.36	1.36	1.34	1.34	1.33	1.31	1.29	1.28	1.34	1.29
11	1.22	1.24	1.21	1.24	1.26	1.27	1.26	1.24	1.24	1.22	1.41	1.37	1.33	1.33	1.32	1.32	1.30	1.29	1.27	1.26	1.31	1.27
12	1.20	1.22	1.19	1.23	1.24	1.25	1.25	1.23	1.22	1.21	1.38	1.34	1.31	1.31	1.29	1.29	1.28	1.27	1.25	1.24	1.29	1.25
13	1.19	1.21	1.18	1.21	1.22	1.23	1.23	1.21	1.21	1.19	1.35	1.32	1.29	1.29	1.27	1.27	1.26	1.25	1.24	1.23	1.27	1.23
14	1.17	1.19	1.17	1.20	1.21	1.22	1.21	1.20	1.19	1.18	1.33	1.30	1.27	1.27	1.26	1.25	1.24	1.23	1.22	1.21	1.25	1.21
15	1.16	1.18	1.16	1.18	1.20	1.20	1.20	1.18	1.18	1.17	1.31	1.28	1.25	1.25	1.24	1.24	1.23	1.22	1.21	1.20	1.24	1.20
16	1.15	1.17	1.14	1.17	1.18	1.19	1.19	1.17	1.17	1.16	1.29	1.26	1.24	1.24	1.22	1.22	1.21	1.20	1.19	1.18	1.22	1.19
17	1.14	1.16	1.14	1.16	1.17	1.18	1.17	1.16	1.16	1.15	1.27	1.24	1.22	1.22	1.21	1.21	1.20	1.19	1.18	1.17	1.21	1.17
18	1.13	1.15	1.13	1.15	1.16	1.17	1.16	1.15	1.15	1.14	1.25	1.22	1.20	1.20	1.19	1.19	1.18	1.18	1.17	1.16	1.19	1.16
19	1.12	1.14	1.12	1.14	1.15	1.15	1.14	1.13	1.13	1.13	1.23	1.21	1.19	1.19	1.18	1.18	1.17	1.16	1.16	1.15	1.18	1.15
20	1.11	1.13	1.11	1.13	1.14	1.14	1.14	1.13	1.12	1.12	1.21	1.19	1.17	1.17	1.17	1.16	1.16	1.15	1.14	1.14	1.16	1.14
21	1.10	1.11	1.10	1.11	1.12	1.13	1.13	1.11	1.11	1.11	1.19	1.17	1.16	1.16	1.15	1.15	1.14	1.14	1.13	1.13	1.15	1.13
22	1.09	1.10	1.09	1.10	1.11	1.11	1.11	1.10	1.10	1.09	1.17	1.15	1.14	1.14	1.13	1.13	1.13	1.12	1.12	1.11	1.13	1.11
23	1.08	1.09	1.07	1.09	1.09	1.10	1.10	1.09	1.09	1.08	1.15	1.13	1.12	1.12	1.12	1.11	1.11	1.11	1.10	1.10	1.11	1.10
24	1.06	1.07	1.06	1.07	1.08	1.08	1.08	1.07	1.07	1.07	1.12	1.11	1.10	1.10	1.09	1.09	1.09	1.09	1.08	1.08	1.09	1.08

Table III
The gap function $\phi(\mathbf{k}, n)$ (up to a multiplicative factor) for 22 IFS pieces (horizontal). 25 non-negative Matsubara frequencies (vertical) are considered ($n_c = 24$)

n	1	2	3	4	5	6	7	8	9	10	11	12	13	14	15	16	17	18	19	20	21	22
0	.50	.58	.47	.58	.66	.70	.67	.62	.60	.55	1.00	.89	.78	.80	.81	.78	.76	.76	.73	.71	.81	.71
1	.44	.51	.40	.51	.58	.61	.59	.55	.52	.49	.89	.79	.69	.70	.68	.68	.65	.62	.58	.56	.68	.57
2	.35	.41	.31	.41	.47	.49	.48	.45	.42	.39	.72	.63	.55	.55	.52	.53	.50	.46	.42	.40	.51	.41
3	.26	.31	.22	.31	.36	.38	.37	.35	.32	.29	.56	.48	.41	.40	.37	.39	.37	.31	.28	.26	.37	.27
4	.18	.23	.15	.22	.27	.28	.27	.26	.23	.21	.41	.35	.29	.28	.25	.28	.25	.20	.17	.16	.25	.17
5	.11	.16	.09	.15	.19	.20	.19	.19	.16	.14	.29	.24	.20	.18	.16	.18	.16	.12	.09	.08	.15	.09
6	.06	.10	.04	.09	.13	.14	.13	.13	.11	.08	.20	.15	.12	.11	.09	.11	.09	.05	.03	.02	.08	.03
7	.02	.06	-.00	.05	.09	.09	.08	.08	.06	.04	.12	.09	.06	.05	.03	.05	.04	-.00	-.02	-.03	.03	-.02
8	-.01	.02	-.03	.01	.05	.08	.05	.05	.03	.01	.06	.03	.01	.00	-.01	.01	-.01	-.04	-.06	-.06	-.01	-.06
9	-.03	-.01	-.06	-.02	.02	.02	.02	.02	-.00	-.02	.02	-.01	-.03	-.04	-.05	-.03	-.04	-.07	-.08	-.09	-.05	-.08
10	-.05	-.03	-.07	-.04	-.00	.00	-.01	-.00	-.02	.04	-.02	-.04	-.06	-.07	-.07	-.06	-.06	-.09	-.11	-.11	-.07	-.10
11	-.07	-.04	-.09	-.06	-.02	-.02	-.03	-.02	-.04	.05	-.05	-.07	-.08	-.09	-.09	-.08	-.08	-.11	-.12	-.12	-.09	-.12
12	-.08	-.06	-.10	-.07	-.03	-.03	-.04	-.04	-.05	.06	-.07	-.09	-.10	-.11	-.11	-.09	-.10	-.12	-.13	-.13	-.11	-.13
13	-.09	-.07	-.11	-.08	-.05	-.05	-.05	-.05	-.06	.07	-.09	-.10	-.12	-.12	-.12	-.11	-.11	-.14	-.15	-.14	-.12	-.14
14	-.10	-.08	-.12	-.09	-.06	-.06	-.06	-.06	-.07	.08	-.10	-.12	-.13	-.13	-.13	-.12	-.12	-.14	-.15	-.15	-.13	-.15
15	-.10	-.08	-.12	-.10	-.06	-.06	-.07	-.06	-.08	.09	-.12	-.13	-.14	-.14	-.14	-.13	-.13	-.15	-.16	-.16	-.14	-.16
16	-.11	-.09	-.13	-.10	-.07	-.07	-.08	-.07	-.09	.10	-.13	-.14	-.15	-.15	-.15	-.13	-.14	-.16	-.17	-.16	-.15	-.16
17	-.11	-.09	-.13	-.11	-.07	-.07	-.08	-.07	-.09	.10	-.14	-.15	-.16	-.16	-.16	-.14	-.14	-.16	-.17	-.17	-.15	-.17
18	-.12	-.10	-.14	-.11	-.08	-.08	-.09	-.08	-.09	.10	-.14	-.15	-.16	-.16	-.16	-.14	-.14	-.16	-.17	-.17	-.16	-.17
19	-.12	-.10	-.14	-.11	-.08	-.08	-.09	-.08	-.10	.11	-.14	-.15	-.16	-.16	-.16	-.15	-.15	-.17	-.18	-.17	-.16	-.17
20	-.12	-.10	-.14	-.12	-.08	-.08	-.09	-.08	-.10	.11	-.15	-.15	-.16	-.16	-.16	-.15	-.15	-.17	-.18	-.17	-.16	-.17
21	-.12	-.10	-.14	-.12	-.09	-.09	-.09	-.08	-.10	.11	-.15	-.16	-.17	-.17	-.17	-.15	-.15	-.17	-.18	-.18	-.16	-.17
22	-.12	-.11	-.14	-.12	-.09	-.09	-.10	-.09	-.10	.11	-.15	-.16	-.17	-.17	-.17	-.15	-.16	-.17	-.18	-.18	-.16	-.17
23	-.12	-.11	-.14	-.12	-.09	-.09	-.10	-.09	-.10	.11	-.15	-.16	-.17	-.17	-.17	-.15	-.16	-.17	-.18	-.18	-.16	-.17
24	-.12	-.11	-.14	-.12	-.09	-.09	-.10	-.09	-.10	.11	-.15	-.16	-.17	-.17	-.17	-.15	-.16	-.17	-.18	-.18	-.16	-.17

Table IV

The groups formed out of the original 22 pieces, reducing their number.

Number	{1}	{2}	{3}	{4}	{9}	{10}	{18}	{19}	{20}	{22}	{5}	{6}	{7}	{8}	{13}	{14}	{16}	{17}	{21}	{11}	{12}
22	{1}	{2}	{3}	{4}	{9}	{10}	{18}	{19}	{20}	{22}	{5}	{6}	{7}	{8}	{13}	{14}	{16}	{17}	{21}	{11}	{12}
11	{1 3}	{2 9}	{3 3}	{4 10}	{9 9}	{10 10}	{18 18}	{19 20}	{20 22}	{22 22}	{5 6}	{6 7}	{7 7}	{8 8}	{13 13}	{14 14}	{16 16}	{17 17}	{21 21}	{11 11}	{12 12}
8	{1 3 3}	{2 9 9}	{3 3 3}	{4 10 10}	{9 9 9}	{10 10 10}	{18 18 18}	{19 20 20}	{20 22 22}	{22 22 22}	{5 6 6}	{6 7 7}	{7 8 8}	{8 8 8}	{13 14 14}	{14 16 16}	{16 15 15}	{17 17 17}	{21 21 21}	{11 11 11}	{12 12 12}
6	{1 3 3}	{2 9 9}	{3 3 3}	{4 10 10}	{9 9 9}	{10 10 10}	{18 18 18}	{19 20 20}	{20 22 22}	{22 22 22}	{5 6 6}	{6 7 7}	{7 8 8}	{8 8 8}	{13 14 14}	{14 16 16}	{16 15 15}	{17 17 17}	{21 21 21}	{11 11 11}	{12 12 12}
4	{1 3 3}	{2 9 9}	{3 3 3}	{4 10 10}	{9 9 9}	{10 10 10}	{18 18 18}	{19 20 20}	{20 22 22}	{22 22 22}	{5 6 6}	{6 7 7}	{7 8 8}	{8 8 8}	{13 14 14}	{14 16 16}	{16 15 15}	{17 17 17}	{21 21 21}	{11 11 11}	{12 12 12}
2	{1 3 3}	{2 9 9}	{3 3 3}	{4 10 10}	{9 9 9}	{10 10 10}	{18 18 18}	{19 20 20}	{20 22 22}	{22 22 22}	{5 6 6}	{6 7 7}	{7 8 8}	{8 8 8}	{13 14 14}	{14 16 16}	{16 15 15}	{17 17 17}	{21 21 21}	{11 11 11}	{12 12 12}
1	{1 3 3}	{2 9 9}	{3 3 3}	{4 10 10}	{9 9 9}	{10 10 10}	{18 18 18}	{19 20 20}	{20 22 22}	{22 22 22}	{5 6 6}	{6 7 7}	{7 8 8}	{8 8 8}	{13 14 14}	{14 16 16}	{16 15 15}	{17 17 17}	{21 21 21}	{11 11 11}	{12 12 12}

Those averaged parameters, and others [10] were used for the isotropic Eliashberg equation solution of Allen and Dynes (their logarithmic factor in μ^* is replaced by the more accurate numeric integration over the $E(n_c)$ function given in equation (2c)). Comparing the obtained T_c and our previous results, the 'total' anisotropy effect turns again to be an increase in T_c , but it is dependent on the cut-off frequency. The increase varies from 0.33°K for $n_c = 6$, through 0.26°K for $n_c = 13$ to 0.21°K for the infinite n_c limit. This variation is due to phonon-anisotropy.

Additional calculation was to change the electron-phonon coupling and the phonon energies by multiplicative factors and to study then the anisotropy effect. Dividing the electron-phonon coupling by 0.7 (which brings us back to the original electron-phonon coupling constants) yields $T_c = 24.91^\circ\text{K}$, a (total) anisotropy effect of 0.30°K and McMillan's T_c of 22.9°K. Multiplying the phonon energies by 0.7 yields $T_c = 17.66^\circ\text{K}$ an anisotropy effect of 0.20°K and McMillan's T_c of 16.2°K (a multiplicative factor for the phonon energies is useful to calculate the isotope effect). McMillan's result is found to deviate considerably for high T_c as was argued by Allen and Dynes.

5. Conclusion

We presented here a method for solving the Eliashberg equations. The method was applied for Nb, and a calculation for any other material is straightforward provided that its band structure and phonon spectrum are known. The computer time required for the calculation was found reasonable, and most of it spent on evaluation of numbers for the construction of the equations rather than on their solution. This suggests that instead of performing rather an elaborate calculation of averaged quantities as McMillan's parameters, one can without substantial increase in the computer time solve the whole Eliashberg problem. One can also test various simplifying models and semiempirical formulas when the exact solution is at hand.

The tight-binding parametrization method has been used for the evaluation of electron-phonon coupling constants. The linear methods for band calculation of Andersen [23] could form a basis for a more accurate calculation of those constants, and perhaps also of the Coulomb interaction constants which were parametrized here. The electron-phonon and the Coulomb parameters can also be tested experimentally through elastic constants and susceptibility measurements.

The method can also be generalized to include the effect of magnetic fields [5] and impurities [24]. It can also be used to calculate the mass renormalization and gap functions on the real frequency axis which can be compared with tunneling experiments results.

The anisotropy effect on T_c was found to be rather small for Nb. However, for materials with lower dimensional characteristics such as the layered compounds, the A15 and the Chevrel phases [25], an unrestricted solution of the Eliashberg equations seems to be essential.

Acknowledgement

The authors would like to acknowledge the contributions of G. Adam, P. Entel and W. Klose in the previous stages of this work. We also benefited from discussions with M. Weger and O. K. Andersen.

References

- [1] Y. NAMBU, Phys. Rev. *117*, 648 (1960).
- [2] G. M. ELIASHBERG, Soviet Phys. JETP *11*, 696 (1960).
- [3] D. J. SCALAPINO, J. R. SCHRIEFFER and J. W. WILKINS, Phys. Rev. *148*, 263 (1966).
- [4] M. PETER, W. KLOSE, G. ADAM, P. ENTEL and E. KUDLA, Helv. Phys. Acta *47*, 807 (1974).
- [5] P. ENTEL and M. PETER, J. Low Temp. Phys. *22*, 613 (1976).
- [6] M. PETER and G. ADAM, Rev. Roum. Phys. *21*, 385 (1976).
- [7] W. L. McMILLAN, Phys. Rev. *167*, 331 (1968).
- [8] A. BIRNBOIM and H. GUTFREUND, Phys. Rev. *B12*, 2682 (1975).
- [9] J. APPEL and W. KOHN, Phys. Rev. *B4*, 2162 (1971).
- [10] P. B. ALLEN and R. C. DYNES, Phys. Rev. *B12*, 905 (1975), and references therein.
- [11] W. H. BUTLER and P. B. ALLEN, Proceedings to the second Rochester Conference on *d*- and *f*-Band Superconductors (Rochester New York 1976).
- [12] J. H. WILKINSON, *The Algebraic Eigenvalue Problem* (Clarendon Press, Oxford 1965).
- [13] L. F. MATTHEISS, Phys. Rev. *B1*, 373 (1970).
- [14] J. ASHKENAZI and M. WEGER, J. Phys. Chem. Sol. *33*, 631 (1971).
- [15] A. BIRNBOIM, Phys. Rev. *B 14*, 2857 (1976).
- [16] J. A. MORIARTY, J. Phys. F *5*, 873 (1975).
- [17] A. BIRNBOIM and H. GUTFREUND, J. Phys. F (to be published).
- [18] D. G. PETTIFOR, J. Phys. C *2*, 1051 (1969); *ibid* *5*, 97 (1972).
- [19] Y. NAGAKAWA and A. D. B. WOODS, *Lattice Dynamics*, edited by R. F. Wallis (Pergamon Press 1963).
- [20] J. ASHKENAZI and M. WEGER, J. Physique *37*, C4-189 (1976).
- [21] H. WATANABE, *Operator Methods in Ligan Field Theory* (New Jersey Prentice-Hall 1960), p. 108.
- [22] P. MOREL and P. W. ANDERSON, Phys. Rev. *125*, 1263 (1962).
- [23] O. KROGH ANDERSEN, Phys. Rev. *B12*, 3060 (1975).
- [24] P. ENTEL, Z. Phys. B *23*, 321 (1976).
- [25] Ø. FISCHER, H. JONES, G. BONGI, M. SERGENT and R. CHEVREL, J. Phys. C *7*, L450 (1974).